Biosensors and Bioelectronics 26 (2011) 1871–1875

Contents lists available at ScienceDirect

Biosensors and Bioelectronics

journal homepage: www.elsevier.com/locate/bios

Prostate specific antigen detection in patient sera by fluorescence-free BioCD protein array

Xuefeng Wang[a], Ming Zhao[a], David D. Nolte[a,*], Timothy L. Ratliff[b]

[a] Department of Physics, 525 Northwestern Avenue, West Lafayette, IN 47907-2036, United States
[b] Purdue Cancer Center, Hansen Life Sciences Research Building, West Lafayette, IN 47907-2064, United States

ARTICLE INFO

Article history:
Received 8 December 2009
Received in revised form 10 February 2010
Accepted 12 February 2010
Available online 20 February 2010

Keywords:
BioCD
Label-free
Interferometry
Antibody microarray
Prostate specific antigen
Cancer biomarker
Serum
Optical biosensor

ABSTRACT

Fluorescence-free biosensor arrays for protein detection directly measure the protein surface density, and do not require a fluorophore or enzyme label, and provide quantitative and consistent signals. However, few fluorescence-free biosensor protein arrays have demonstrated successful application in high-background samples, such as serum, due to non-specific binding. We tested the BioCD as a fluorescence-free biosensor based on optical interferometry, and used it to detect prostate specific antigen (PSA, a biomarker of prostate cancer) in patient sera in a 96-well anti-PSA microarray. We have attained a 4 ng/ml detection limit in serum and have measured PSA concentrations in patient sera. The measured concentrations correlated well with enzyme-linked immunosorbent assay (ELISA) results. The measurement of PSA concentrations in high-level protein backgrounds suggests that the BioCD has a potential for clinical applications by removing the restriction of fluorescence-free biosensors from high-background applications.

1. Introduction

The development of fluorescence-free biosensors for protein detection (without the need for fluorophore labeling or radiolabels) is advancing rapidly (Fan et al., 2008). Surface plasmon resonance (SPR) (Anker et al., 2008; Homola et al., 1999; Willets and Van Duyne, 2007), imaging ellipsometry (Jin et al., 1995; Malmsten, 1994), photonic gratings (Cunningham et al., 2002), reflectometry (Gao and Rothberg, 2007; Lu et al., 2004; Mace et al., 2008) BioCD (Varma et al., 2004; Wang et al., 2007, 2008a, 2009; Zhao et al., 2007), nanowires (Zheng et al., 2005), and micro-cantilevers (Burg et al., 2007; Wee et al., 2005) have been proposed and demonstrated in succession. These biosensors sense the surface density of biomaterial and have the potential for high-throughput and quantitative protein detection. Methods such as Western blot or enzyme-linked immunosorbent assay (ELISA) detect specific protein via fluorescence or other chemically induced signals. These signals are assumed to be proportional to the amount of target protein. However, the intensity of fluorescence and the chemically induced signals may be adversely affected by other parameters, such as local electrical field intensity, pH, temperature, or may be subject to bleaching and quenching. On the other hand, fluorescence-free biosensors measure protein quantity by directly converting the protein areal density into physical signals which are less dependent on the local micro-environment. For example, SPR, ellipsometry and the BioCD convert protein amount (specifically optical dipole density) into optical quantities (reflectance, polarization and light intensity, respectively). Nanowires and micro-cantilevers convert protein mass into electrical and mechanical quantities, respectively. Among these biosensors, the BioCD converts protein surface density on a SiO_2/Si wafer into a reflectance variation via local interferometry which maximizes the protein signal using a phase-quadrature condition (Zhao et al., 2006). The large area of the wafer can accommodate thousands of assays simultaneously. SiO_2/Si wafers can be obtained economically, and the SiO_2 modification has been extensively studied for protein immobilization. In addition, the BioCD scanning system adopts a spinning-disc approach which reduces the detection noise floor by high-speed repetitive sampling and improves protein detection limits.

Protein array surface density biosensors face obstacles in clinical applications because the background protein level in serum is much higher than the target protein concentration and induces strong non-specific binding. Non-specific binding can mask the target signal because label-free biosensors detect all protein bound rather than only the specific target protein. In this report, we adopted an enhanced Schiff-base method to produce butyraldehyde-modified

* Corresponding author. Tel.: +1 765 494 3103.
E-mail address: nolte@physics.purdue.edu (D.D. Nolte).

0956-5663/$ – see front matter © 2010 Published by Elsevier B.V.
doi:10.1016/j.bios.2010.02.009

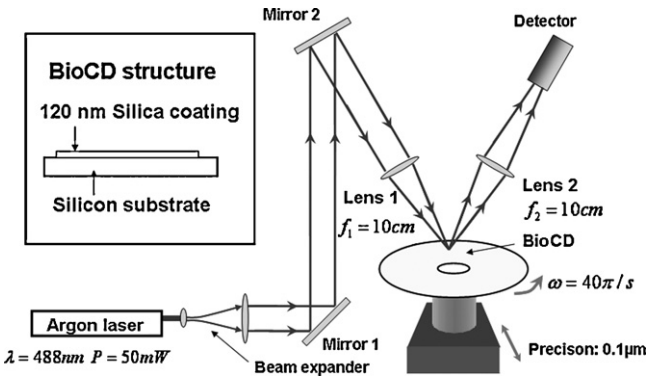

Fig. 1. BioCD scanning system. The system scans the BioCD and acquires a 2D reflectance map with 20 μm transverse resolution. The probe light with 488 nm wavelength is incident obliquely to achieve an optimal interferometric condition for protein sensing on 120 nm thermal oxide silicon wafers.

silicon wafers for an antibody microarray that significantly suppresses non-specific binding. The high sensitivity of the BioCD combined with stable surface chemistry allows us to detect the target protein at ng/ml levels in a high protein background, such as serum (total protein level > 40 mg/ml (Wadsworth and Oliveiro, 1953)).

2. Materials and methods

2.1. Principle of the BioCD

The BioCD is a disc with a simple single-layer dielectric coating (Nolte, 2009). The coating creates a surface reflection coefficient r and reflectance $R = |r|^2$. After a protein layer is immobilized on the coating surface, the reflectance is changed to R'. We have shown previously (Wang et al., 2008b) that the reflectance increment caused by protein, $\Delta R = R' - R$, has an explicit relation to the original r, expressed by

$$\Delta R = Im[(1+r)^2 \tilde{r}]\ (n_p^2 - 1)\ \frac{2\pi d}{\lambda \cos\ \theta_0} \quad (1)$$

where n_p is the refractive index of the protein layer, d is the thickness of the protein layer, λ is the wavelength of the probe light, and θ_0 is the incident angle. A laser scans the disc, measuring the height (or mass area density) of printed protein. For a defined protein layer and probe wavelength, where n_p, d, λ and θ_0 are constants, ΔR is maximized when $r = \pm 0.577i$. A silicon wafer with 120 nm of thermal SiO_2 has a calculated $r = -0.049 + 0.489i$ at a wavelength of 488 nm with s-polarization and 30° incidence, which is near the optimal value for r. This working condition requires only one dielectric layer (SiO_2). On this 120 nm SiO_2 wafer, a 1 nm saturated protein layer induces 0.0056 absolute reflectance change, or 2.3% relative intensity increment. A spinning-disc scanning system acquires the reflectance map of the entire disc, which is converted into a map of protein dipole density expressed as an average protein layer height.

2.2. Scanning system

The experimental layout of the BioCD scanning system is shown in Fig. 1. The probe light is incident at 30° on the disc with s-polarization to optimize the performance on the 120 nm thermal oxide silicon wafer. However, unpolarized normally incident light would work as well for a different thermal oxide thickness of 115 nm. The light source is an INNOVA 300 Argon laser (Coherent, Inc.) at a wavelength of 488 nm. The reflectance signal of the BioCD is detected by a silicon-based detector. The BioCD is mounted on a motor (Lincoln Laser, Inc.) on a linear translation stage (MM2000, Newport Corp). The 2D scanning is performed by spinning the motor and moving the stage. A computer controls the system, collects the reflectance data and reconstructs the reflectance map of the entire BioCD with a lateral resolution of 20 μm. One scan of a 100 mm diameter BioCD is completed in 60 min. The reflectance map is converted to a protein thickness profile using the conversion ratio d (nm) = $\Delta R/R/0.023$, where R is the background reflectance, and ΔR is the reflectance change caused by the protein layer.

2.3. Surface chemistry

The 120 nm thermal oxide on silicon was aldehyde-functionalized to bind protein covalently. Butyraldehyde was grafted onto the SiO_2 surface through silanization (Fig. 2). Before silanization, the silicon wafer is immersed in 10% NaOH (in water) for 12 h at room temperature, rinsed in water, rinsed in 1% HCl, and rinsed in water again and spun dry. For the silanization, 5% water and 2% triethoxysilylbutyraldehyde (TESBA) (GELEST Co.) are mixed into ethanol. The TESBA solution is stirred for 3 min at room temperature. And the cleaned wafer is immersed in the solution for 3 min at room temperature. The wafer is rinsed in pure ethanol and spun dry (MacBeath, 2007). After the silianization, the silanol group (Si–OH) on the aldehydic silane reacts with a hydroxyl group (–OH) on hydrated silica surface and forms a disiloxane bond (Si–O–Si). The antibodies were printed on the functionalized silica surface by a piezoelectric protein printer. The carbonyl group of butyraldehyde reacts with the amino groups of the antibody to form a Schiff base (MacBeath and Schreiber, 2000), a carbon–nitrogen double bond which immobilizes the antibody molecules through primary amines. After antibody printing, the surface was reduced by a $NaBH_4$ solution (1.0 g $NaBH_4$ in 300 ml phosphate buffered saline (PBS) + 100 ml ethanol). The wafer is incubated in $NaBH_4$ solution for 15 min at room temperature and then rinsed by PBS solution. $NaBH_4$ solution stabilizes antibody attachment by converting carbon–nitrogen double bonds (C=N) to carbon–nitrogen single bonds (C–N). The $NaBH_4$ also helps to block the substrate by reducing remnant carbonyl groups to hydroxyl groups. The BioCD is further blocked by casein solution (PBS + 1% casein solution in 20:1 volume ratio, pH 8.0), washed by 50 mM citric acid solution (pH 6.0), PBST (PBS + 0.05% Tween 20) and deionized water and spun dry at 1000 rpm. Bovine serum albumin (BSA) is widely used for surface blocking in many antibody microarrays, but it is not recommended for

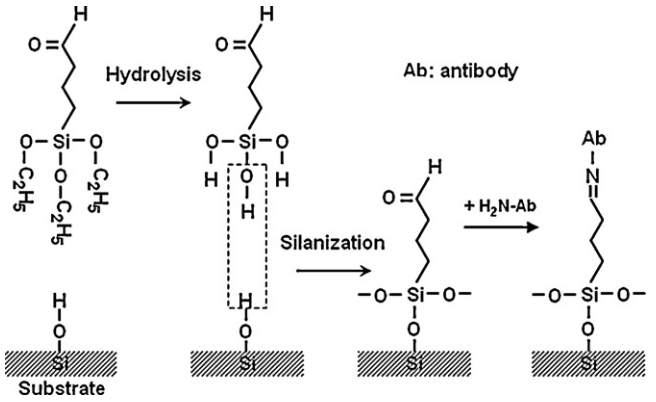

Fig. 2. Aldehyde modification of SiO_2 surface and antibody immobilization. (1) Triethoxysilylbutyraldehyde (TESBA) is hydrolyzed and generates silanol groups which react with the hydroxyl group on SiO_2 surface and forms a disiloxane bond which attaches butyraldehyde on the surface. (2) The carbonyl group of butyraldehyde reacts with the amino groups of the antibody to form a carbon–nitrogen double bond which immobilizes the antibody molecules through primary amines.

the mass-sensing BioCD because BSA is a large protein molecule (molecular weight = 70 kDa) which contributes more mass noise for interferometric biosensors. Here, we use casein for its small molecular weight (molecular weight is around 20 kDa).

2.4. Prostate specific antigen (PSA)

We applied the BioCD to detect PSA levels in prostate cancer patient sera. PSA is a member of the kallikrein family exclusively produced by the prostate gland. It has a concentration of 0.5–2.0 mg/ml in normal seminal fluid (Lovgren et al., 1999; Wang et al., 1981) and 0–4 ng/ml (Catalona et al., 1994) in normal serum. Prostate cancer and other prostate pathological changes may cause PSA to leak into the peripheral circulation and induce an abnormal elevation of PSA in serum. Levels higher than 4 ng/ml may suggest the presence of prostate cancer. Therefore PSA can work as a biomarker for prostate cancer. Measurement of PSA in serum is one of the standard diagnostics for prostate cancer and usually is performed by ELISA. There has been no previous study showing successful PSA measurement in patient sera based on mass-sensing biosensors in a microarray format.

2.5. 96-well BioCD

We print antibody and reference protein in the format of paired target and reference spots in a 2×2 spot unit cell layout on the BioCD (shown in Fig. 3d). A prescan records the initial height of all protein spots. During analyte solution incubation, antibodies capture target antigen due to immuno-binding, and the height of the antibody spot increases. In a sandwich assay, a second primary antibody binds to the captured antigen and increases the spot height further, which is measured by a postscan after the assay. The specific height increment is defined as the antibody increment minus the reference-spot increment. If non-specific binding is similar on both spots, then this procedure subtracts this background contribution, and the difference is related to the antigen concentration in the sample. Together – printing antibody, a prescan, incubation of analyte solution followed by a second specific antibody, and a postscan – complete one assay. To perform multiple assays simultaneously on a single BioCD, the surface of a 100 mm diameter disc is separated into 96 wells with ultra-hydrophobic surface pads shown in Fig. 3(a–c). The contact angle of water on the pads is as large as 90° and confines the incubation solution within each well so that 96 assays can be performed in parallel on a single disc.

The 96-well BioCD enables multiple sample tests or multiplexed protein detection, respectively, by incubating with different samples or by printing multiplexed antibodies in wells. Fig. 3 shows the prescan of a 96-well anti-PSA BioCD used in the experiment. The protein thickness profile is derived from the reflectance map and recorded for each well, as shown in Fig. 3(d). An assay example is shown in Fig. 4 in which a negative and a positive response were observed, respectively, for 0 and 1 μg/ml analyte incubation.

3. Experiments and results

3.1. Non-fluorescent assay in patient sera based on 96-well BioCD

We applied the 96-well anti-PSA BioCD to PSA detection in sera from three prostate cancer patients. A Scienion (BioDot Corp.) piezoelectric printer was used to print 32 antibody spots (affinity-purified polyclonal anti-PSA produced in goat, G-126-C, Biospacific Co.) and 32 reference spots (anti-rabbit IgG produced in goat, R2004, Sigma Inc.) in each of the 96 wells on a butyraldehyde-activated BioCD. The printed antibody concentrations were 100 μg/ml, and each spot was printed with a volume of 2.5 nl. Post-print incubation time was 2 h (in 100% humidity cham-

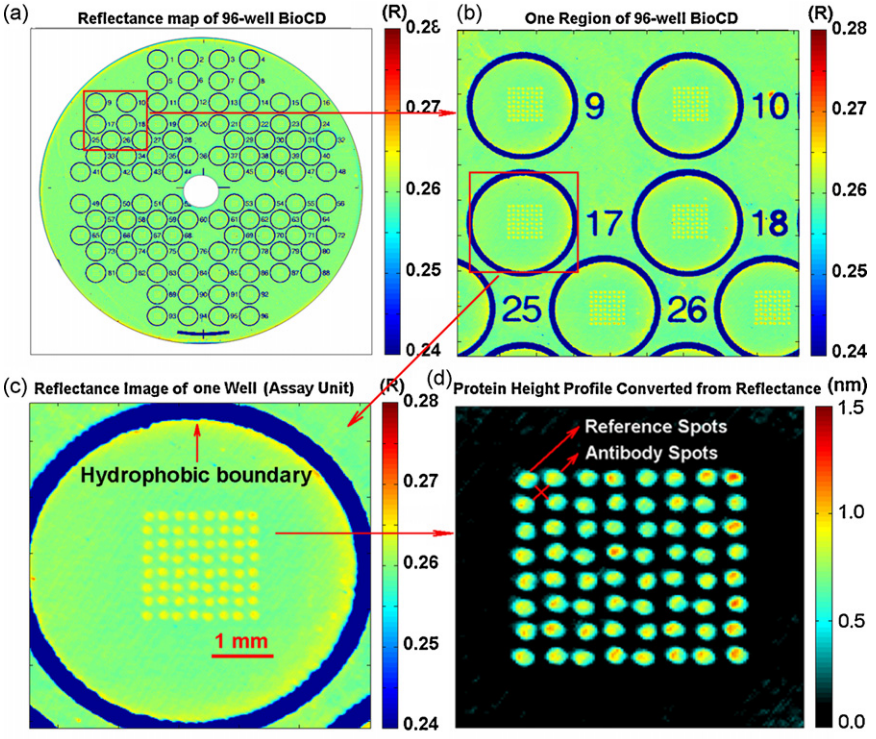

Fig. 3. Images of protein profiles on a 96-well BioCD. (A and B) 96 wells were isolated and numbered with ultra-hydrophobic ink on a thermal oxide silicon wafer with 120 nm SiO_2. (C) Antibody and reference spots were printed in wells in an 8×8 spot pattern consisting of 2×2 unit cells of two target and two reference spots. Incubation solution is confined within each single well by the hydrophobic boundary, allowing multiple sample tests to be performed on a single BioCD. (D) Protein spot mass profile (protein layer height in units of nm) of each well derived from the reflectance map.

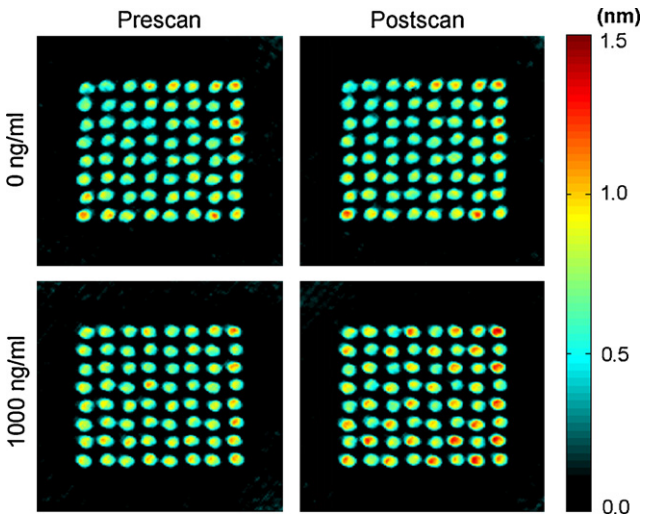

Fig. 4. Demonstration of two well-based sandwich assays at 0 and 1000 ng/ml. A prescan was performed before the assays to record the original height of the protein spots. After the sandwich assays, a postscan recorded the new protein heights. For the well incubated with 0 ng/ml PSA spiked in female serum, the average specific increment is 0.007 ± 0.01 nm (spot-to-spot error), and for the well incubated by 1000 ng/ml PSA spiked into serum, the increment is 0.18 nm.

ber to prevent water evaporation). The diameter of each spot was approximately 150 μm with a spot-to-spot separation of approximately 300 μm. Each antibody spot was locally paired with a reference spot in a 2×2 unit cell format, as shown in Fig. 3(d). A prescan was performed to record the original protein profile of the entire BioCD after printing.

Test samples included: (1) female serum (PSA level is null in female serum for a negative control), (2) PSA spiked into female serum, and (3) prostate cancer patient sera. The three patient sera were acquired from the Purdue Cancer Center. The PSA concentrations had been measured with ELISA to be 30, 120 and 2100 ng/ml, respectively, for samples 1, 2 and 3. Female serum was purchased from Innovative Research, Inc. Affinity-purified PSA reagent was purchased from Fitzgerad Co.

We created a concentration series of PSA-spiked female sera with PSA concentrations 0, 4, 12.6, 40, 126, 400, 1260, 4000, and 12,640 ng/ml. The PSA-spiked serum was used to generate a standard PSA response curve. For all three patient sera, we performed a series dilution in half-logarithmic sequential ratios 1:1, 1:3.16, 1:10, 1:31.6, 1:100 diluted by female serum. Dilution with female serum instead of buffer solution maintains an equal protein background for all test samples.

Prior to incubation, all samples were diluted by PBST solution in a ratio 1:4. This step is crucial because Tween-20 in the buffer suppresses non-specific binding. All samples shared the same protein background level (i.e., 1/4 of full human serum) at about 10 mg/ml. Patient sera dilution ratios then became 1:4, 1:12.6, 1:40, 1:126 and 1:400. PSA concentrations in spiked female serum became 0, 1, 3.16, 10, 31.6, 100, 316, 1000, 3160 ng/ml. We incubated the 96-well anti-PSA BioCD with these prepared samples. Each sample was distributed across 4 randomly allotted wells to suppress local bias on the disc. Overall, 9×4 wells were used for PSA spiked serum to acquire the standard response curve, and $3 \times 5 \times 4$ wells were used for diluted patient sera to acquire the curves for sequential dilution. The incubation time was 1 h, after which the BioCD was washed for 5 min with PBST and 5 min with DI water (on an orbital shaker) and dried with pure nitrogen. After this procedure, PSA molecules in the samples had been captured by the anti-PSA spots on the BioCD.

Sandwich assays were performed to enhance the assay response through the added mass of the second antibody. All 96 wells were incubated with 10 μg/ml anti-PSA (G-126-C, Biospacific Co.) in PBST for 30 min (static incubation), followed by 5 min PBST and 5 min DI water wash (on orbital shaker), and dried with pure nitrogen. The anti-PSA antibodies bind with the captured PSA antigen and increase the antibody spot height in the assays. A postscan was performed to record all protein spot heights after the sandwich incubation.

The immunoassay responses in all wells were computed from the prescan and postscan data of the 96-well BioCD reflectance map (with a transverse resolution of 20 μm and a height sensitivity of 10 pm (spot-to-spot error)). An image analysis program located all wells on the map, extracted protein spot profiles for each well and calculated the pre- and post-height of all 6144 spots. The assay response was then calculated for each pair of antibody and reference spots by the algorithm $(\text{postH}-\text{preH})_{\text{antibody}} - (\text{postH}-\text{preH})_{\text{reference}}$. The analysis can be completed in less than 10 min on a desktop computer.

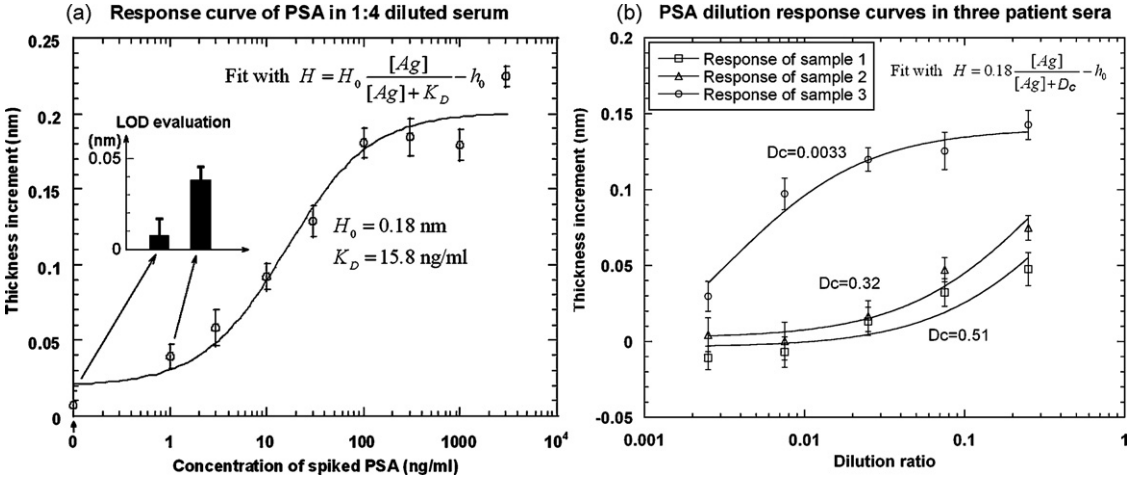

Fig. 5. PSA concentration recovery for three patient samples. We compared and matched the dilution curves shown in (b) with the standard response curve in (a) to find the concentration of PSA in the patient sera. The standard curve was acquired from the assay results based on a series of PSA-spiked female sera and fit by a Langmuir equation. The equilibrium constant K_D was 15.8 ng/ml for PSA in serum. The central dilution ratios D_C were 0.51, 0.32, and 0.0033 for the three patient samples. The PSA concentrations are calculated as $[\text{PSA}]=K_D/D_C$ and are 30, 50, 4800 ng/ml, respectively for samples 1, 2 and 3. The PSA levels measured by ELISA in these three samples were 30, 120 and 2100 ng/ml, respectively.

3.2. Evaluation of the detection limit for PSA

We evaluated the limit of detection (LOD) for PSA by comparing the assay responses for 0 and 1 ng/ml PSA spiked sera shown in Fig. 5a (LOD evaluation). The error bars represent the standard error of the assay variation for each test sample using 128 spots as the spot population number (four replicate wells). The assay response is 0.007 ± 0.0094 nm for 0 ng/ml PSA spiked female serum as a negative control sample and 0.039 ± 0.0078 nm for 1 ng/ml PSA spiked female serum. The difference is $0.039 - 0.007 = 0.032$ nm with a standard error $\sqrt{(0.0094)^2 + (0.0078)^2} = 0.012$ nm, making the assay response positive at 1 ng/ml in PSA-spiked female serum (1:4 dilution of full serum) with a background of about 10 mg/ml. The detectable PSA level is 100 ppb of the background concentration. The 1 ng/ml detection limit in 1:4 serum is equivalent to 4 ng/ml in full serum, which is the clinical threshold for prostate cancer diagnosis.

3.3. PSA concentration recovery in patient sera

A standard PSA response curve was generated from the assays of PSA-spiked female sera. The dilution curves of patient samples were acquired from sequentially diluted samples. We measured the PSA levels in the patient sera by matching the effective concentrations of the dilution series. Both the standard response and the dilution curves are fit by the Langmuir equation (Langmuir, 1916) $H = H_{satur}[PSA]/[PSA] + K_D$ and $H = H_{satur}D/D + D_C$ where D is the dilution ratio, K_D is the equilibrium constant, and D_C is the central dilution ratio at which the assay response is the half of the saturated response. K_D and D_C were calculated by fitting the standard response curve and the dilution curves of the patient samples. Because D_C is the dilution ratio at which the diluted sample has the same assay response as a sample with an analyte concentration equal to K_D, the analyte concentration in the test sample is recovered as the ratio K_D/D_C.

The standard response curve and patient sera dilution curves are shown in Fig. 5(a and b). K_D was found to be 15.8 ng/ml, and the D_C are 0.51, 0.32 and 0.0033, respectively, for patient serum samples 1, 2 and 3. The recovered PSA concentrations are 30 ng/ml for sample 1, 50 ng/ml for sample 2 and 4800 ng/ml for sample 3. PSA levels in the three samples were measured previously to be 30, 120 and 2100 ng/ml by ELISA.

4. Conclusions

We have demonstrated a mass-sensing biosensor capable of measuring a low-level cancer biomarker in patient sera. Mass-sensing biosensor protein arrays have been challenged by strong non-specific binding caused by the high protein background in serum. Currently, few mass-sensing biosensor protein arrays can successfully detect target protein in serum and hence are excluded from clinical applications. To suppress the non-specific binding, we used a reference-spot subtraction analysis, Schiff-base reduction, casein blocking and 0.05% Tween 20 in the analyte solution to further suppress non-specific binding. Moreover, the locally paired reference spot for each antibody spot helped to monitor and neutralize the local non-specific binding. The large population of antibody spots further reduced the detection error. The combination of these factors has allowed us to successfully detect PSA in prostate cancer patient sera. We found a 1 ng/ml PSA detection limit in PSA-spiked serum with 10 mg/ml background. This detection limit is equivalent to 4 ng/ml PSA in full serum, which is the threshold for normal-to-abnormal PSA levels. We also recovered the PSA concentrations for three patient serum samples at 31, 49 and 4788 ng/ml by comparing the dilution response curve with the standard response curve. These results suggest that the combination of the BioCD interferometric laser scanning with the enhanced Schiff base chemistry has the potential for clinical applications.

Acknowledgements

This work was sponsored under grants from Quadraspec, Inc., the Indiana Economic Development Corporation through the Purdue Research Foundation, and from NIH grant 5R21CA125336-02.

References

Anker, J.N., Hall, W.P., Lyandres, O., Shah, N.C., Zhao, J., Van Duyne, R.P., 2008. Nature Materials 7 (6), 442–453.
Burg, T.P., Godin, M., Knudsen, S.M., Shen, W., Carlson, G., Foster, J.S., Babcock, K., Manalis, S.R., 2007. Nature 446 (7139), 1066–1069.
Catalona, W.J., Richie, J.P., Ahmann, F.R., Hudson, M.A., Scardino, P.T., Flanigan, R.C., Dekernion, J.B., Ratliff, T.L., Kavoussi, L.R., Dalkin, B.L., Waters, W.B., Macfarlane, M.T., Southwick, P.C., 1994. Journal of Urology 151 (5), 1283–1290.
Cunningham, B., Li, P., Lin, B., Pepper, J., 2002. Sensors and Actuator B: Chemical 81 (2–3), 316–328.
Fan, X.D., White, I.M., Shopoua, S.I., Zhu, H.Y., Suter, J.D., Sun, Y.Z., 2008. Analytica Chimica Acta 620 (1–2), 8–26.
Gao, T., Rothberg, L.J., 2007. Analytical Chemistry 79 (20), 7589–7595.
Homola, J., Yee, S., Gauglitz, G., 1999. Sensors and Actuators B 54, 3–15.
Jin, G., Tengvall, P., Lundstrom, I., Arwin, H., 1995. Analytical Biochemistry 232 (1), 69–72.
Langmuir, I., 1916. Journal of American Chemical Society 38, 2221–2295.
Lovgren, J., Valtonen-Andre, C., Marsal, K., Lilja, H., Lundwall, A., 1999. Journal of Andrology 20 (3), 348–355.
Lu, J.H., Strohsahl, C.M., Miller, B.L., Rothberg, L.J., 2004. Analytical Chemistry 76 (15), 4416–4420.
MacBeath, G., 2007. Cold Spring Harb. Protoc.
MacBeath, G., Schreiber, S.L., 2000. Science 289, 1760–1763.
Mace, C.R., Striemer, C.C., Miller, B.L., 2008. Biosensors and Bioelectronics 24 (2), 334–337.
Malmsten, M., 1994. Journal of Colloid and Interface Science 166, 333–342.
Nolte, D.D., 2009. Review of Scientific Instruments 80, 101101.
Varma, M.M., Inerowicz, H.D., Regnier, F.E., Nolte, D.D., 2004. Biosensors and Bioelectronics 19 (11), 1371–1376.
Wadsworth, G.R., Oliveiro, C.J., 1953. British Medical Journal 2 (4846), 1138–1139.
Wang, M.C., Papsidore, L.D., Kuriyama, M., Valenzuela, L.A., Murphy, G.P., Chu, T.M., 1981. Prostate 2 (1), 89–96.
Wang, X.F., Zhao, M., Nolte, D., 2007. Applied Optics 46 (32), 7836–7849.
Wang, X.F., Zhao, M., Nolte, D.D., 2008a. Biosensors and Bioelectronics 24 (4), 981–987.
Wang, X.F., Zhao, M., Nolte, D.D., 2008b. Applied Physics Letters 93 (22), 223904-1–223904-3.
Wang, X.F., Zhao, M., Nolte, D.D., 2009. Analytical and Bioanalytical Chemistry 393, 1151–1156.
Wee, K.W., Kang, G.Y., Park, J., Kang, J.Y., Yoon, D.S., Park, J.H., Kim, T.S., 2005. Biosensors and Bioelectronics 20 (10), 1932–1938.
Willets, K.A., Van Duyne, R.P., 2007. Annual Review of Physical Chemistry 58, 267–297.
Zhao, M., Cho, W., Regnier, F., Nolte, D., 2007. Applied Optics 46, 6196–6209.
Zhao, M., Nolte, D., Cho, W.R., Regnier, F., Varma, M., Lawrence, G., Pasqua, J., 2006. Clinical Chemistry 52 (11), 2135–2140.
Zheng, G.F., Patolsky, F., Cui, Y., Wang, W.U., Lieber, C.M., 2005. Nature Biotechnology 23 (10), 1294–1301.